

NEW RESULTS AND FUTURE PLANS WITH REAL PHOTONS AT MAMI*

R. BECK, R. LEUKEL AND A. SCHMIDT

for the A2- and TAPS-Collaborations

Institut für Kernphysik, Johannes Gutenberg Universität Mainz
Johann-Joachim-Becher-Weg 45, 55099 Mainz, Germany

(Received January 22, 2002)

The photon asymmetry in the reaction $p(\gamma, \pi^0)p$ has been measured with the photon spectrometer TAPS using linearly polarized photons from the tagged-photon facility at the Mainz Microtron MAMI close to the pion threshold and in the $\Delta(1232)$ -resonance region. The total and differential cross sections were also measured simultaneously with the photon asymmetry. This allowed determination of the S -wave and all three P -wave amplitudes. The results in the threshold region are compared to the predictions of ChPT. With the photon spectrometer TAPS the full polar angular range of the pion could be covered and from the new results in the $\Delta(1232)$ region a E2/M1-ratio of $-(2.4 \pm 0.16_{\text{stat.}} \pm 0.24_{\text{sys.}}) \%$ is extracted.

PACS numbers: 13.60.Le, 14.20.Gk, 13.60.Rj

1. Pion photoproduction in the threshold region

The photoproduction of pions near threshold has been a topic of considerable experimental and theoretical activities over the past years, ever since the results of the experiments, performed in Saclay [1], Mainz ([2, 3]) and Saskatoon [4], were at variance with the prediction of a Low Energy Theorem (LET), which was derived in the early 70's [5, 6]. Being based on fundamental principles, this LET predicted the value of the S -wave threshold amplitude E_{0+} in a power series in $\mu = m_\pi/m_N$, the ratio of the masses of the pion and nucleon.

The discrepancy could be explained by a calculation in the framework of heavy-baryon Chiral Perturbation Theory (ChPT) [7], which showed that additional contributions due to pion loops in μ^2 have to be added to the old LET. Refined calculations within heavy-baryon ChPT [8] led to descriptions

* Presented at the VI TAPS Workshop, Krzyże, Poland, September 9–13, 2001.

of the four relevant amplitudes at threshold by well-defined expansions up to order p^4 in the S -wave amplitude E_{0+} and p^3 in the P -wave combinations P_1 , P_2 and P_3 , where p denotes any small momentum or pion mass, the expansion parameters in heavy-baryon ChPT. To that order, three Low-Energy Constants (LEC) due to the renormalization counter terms appear, two in the expansion of E_{0+} and an additional LEC b_P for P_3 , which have to be fitted to the data or estimated by resonance saturation.

However, two combinations of the P -wave amplitudes, P_1 and P_2 , are free of low-energy constants. Their expansions in μ converge rather well leading to new LETs for these combinations. Therefore, the P -wave LETs offer a significant test of heavy-baryon ChPT. However, for this test the S -wave amplitude E_{0+} and the three P -wave combinations P_1 , P_2 and P_3 have to be separated. This separation can be achieved by measuring the photon asymmetry using linearly polarized photons, in addition to the measurement of the total and differential cross sections.

The differential cross sections can be expressed in terms of the S - and P -wave multipoles, assuming that close to threshold neutral pions are only produced with angular momenta l_π of zero and one. Due to parity and angular momentum conservation only the S -wave amplitude E_{0+} ($l_\pi = 0$) and the P -wave amplitudes M_{1+} , M_{1-} and E_{1+} ($l_\pi = 1$) can contribute and it is convenient to write the differential cross section and the photon asymmetry in terms of the three P -wave combinations $P_1 = 3E_{1+} + M_{1+} - M_{1-}$, $P_2 = 3E_{1+} - M_{1+} + M_{1-}$ and $P_3 = 2M_{1+} + M_{1-}$. The c.m. differential cross section is

$$\frac{d\sigma(\theta)}{d\Omega} = \frac{q}{k}(A + B \cos(\theta) + C \cos^2(\theta)), \quad (1)$$

where θ is the c.m. polar angle of the pion with respect to the beam direction and q and k denote the c.m. momenta of pion and photon, respectively. The coefficients $A = |E_{0+}|^2 + |P_{23}|^2$, $B = 2\text{Re}(E_{0+}P_1^*)$ and $C = |P_1|^2 - |P_{23}|^2$ are functions of the multipole amplitudes with $P_{23}^2 = \frac{1}{2}(P_2^2 + P_3^2)$. Earlier measurements of the total and differential cross sections already allowed determination of E_{0+} , P_1 and the combination P_{23} .

In order to obtain E_{0+} and all three P -waves separately and to test the new LETs of ChPT, it is necessary to measure, in addition to the cross sections, the photon asymmetry Σ ,

$$\Sigma = \frac{d\sigma_\perp - d\sigma_\parallel}{d\sigma_\perp + d\sigma_\parallel}, \quad (2)$$

where $d\sigma_\perp$ and $d\sigma_\parallel$ are the differential cross sections for photon polarizations perpendicular and parallel to the reaction plane defined by the pion and

proton. The asymmetry is proportional to the difference of the squares of P_3 and P_2 :

$$\Sigma(\theta) = \frac{\frac{q}{2k}(P_3^2 - P_2^2) \sin^2(\theta)}{\frac{d\sigma(\theta)}{d\Omega}}. \quad (3)$$

A measurement of the reaction $p(\vec{\gamma}, \pi^0)p$ [9] was performed at the Mainz Microtron MAMI [10] using the Glasgow/Mainz tagged photon facility [11, 12] and the photon spectrometer TAPS [13]. The MAMI accelerator delivered a continuous wave beam of 405 MeV electrons. Linearly polarized photons were produced via coherent bremsstrahlung in a 100 μm -thick diamond radiator [14, 15] with degrees of polarization of up to 50%. The neutral pion decay photons were detected in TAPS [16], an array of 504 BaF₂-detectors, which was built up around a liquid hydrogen target.

The total and differential cross sections were measured over the energy range from π^0 -threshold to 168 MeV. Fig. 1 shows the results for the total cross section in comparison to Ref. [4] and [3]. The results for the photon asymmetry are shown in Fig. 2 in comparison to the values of ChPT [8] and to a prediction of a dispersion theoretical calculation (DR) by Hanstein, Drechsel and Tiator [17]. The photon asymmetry was determined from all the data between threshold and 166 MeV for which the mean energy was 159.5 MeV. The theoretical predictions are shown for the same energy.

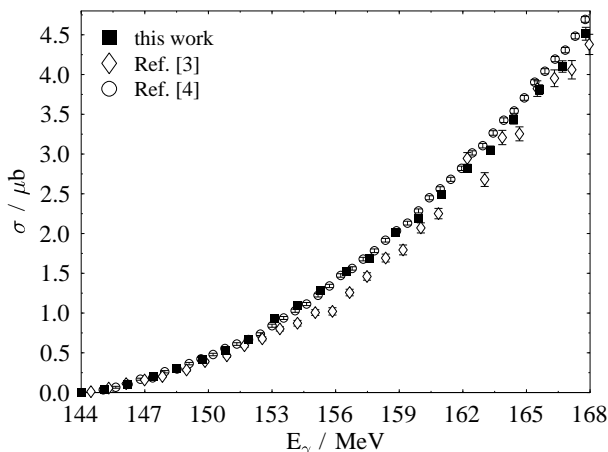


Fig. 1. Total cross sections for π^0 photoproduction close to threshold with statistical errors (without systematic error of 5%) as function of incident photon energy (solid squares, this work Ref. [18], open circles, Ref. [4], open diamonds Ref. [3]).

The values for the real and imaginary part of E_{0+} and the three P -wave combinations were extracted via two multipole fits to the cross sections and the photon asymmetry simultaneously. The two multipole fits differ in the

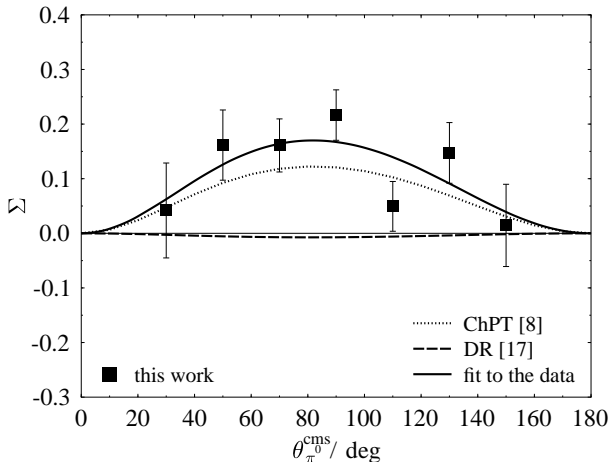


Fig. 2. Photon asymmetry Σ for π^0 photoproduction at 159.5 MeV photon energy with statistical errors (without systematic error of 3 %) as a function of the polar angle θ (solid line: fit to the data) in comparison to ChPT [8] (dotted line) and DR [17] (dashed line).

energy dependence of the real parts of the P -wave combinations. For the first fit the usual assumption of a behaviour proportional to the product of q and k was adopted (qk -fit, $\chi^2/\text{dof} = 1.28$). The assumption made for the second fit is an energy dependence of the P -wave amplitudes proportional to q (q -fit, $\chi^2/\text{dof} = 1.29$). This is the dependence which ChPT predicts for the P -wave amplitudes in the near-threshold region, but at higher energies the prediction is in between the q and qk energy dependence.

The results of both multipole fits for $\text{Re } E_{0+}$ as a function of the incident photon energy are shown in Fig. 3 and compared with the predictions of ChPT and of DR. The results for the threshold values of $\text{Re } E_{0+}$ (at the π^0 - and π^+ -threshold), for the parameter β of $\text{Im } E_{0+}$ and for the values of the threshold slopes of the three P -wave combinations of the qk -fit and the q -fit are summarized in Table I, for more details see [18].

For both fits the low-energy theorems of ChPT ($\mathcal{O}(p^3)$) for P_1 and P_2 agree with the measured experimental results within their systematic and statistical errors. The experimental value for P_3 is higher than the value of ChPT, which can be explained by the smaller total and differential cross sections of Ref. [3], used by ChPT to determine the dominant low-energy constant b_P for this multipole [19]. A new fourth-order calculation in heavy-baryon ChPT by Bernard *et al.*, introduced in [20] and compared to the new MAMI data presented in this letter, shows, that the potentially large Δ -isobar contributions are canceled by the fourth-order loop corrections to the

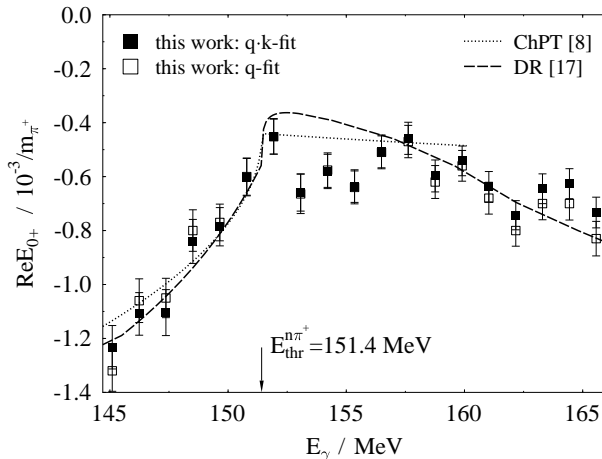


Fig. 3. Results for $\text{Re } E_{0+}$ with statistical errors as a function of incident photon energy E_{γ} for an assumed energy dependence of the P -wave amplitudes proportional to qk (solid squares) and q (open squares) in comparison to ChPT [8] (dotted line) and DR [17] (dashed line).

TABLE I

Results of both fits (qk -fit and q -fit) for $\text{Re } E_{0+}$ at the π^0 - and π^+ -threshold (unit: $10^{-3}/m_{\pi^+}$), for the parameter β of $\text{Im } E_{0+}$ (unit: $10^{-3}/m_{\pi^+}^2$) and for the three combinations of the P -wave amplitudes (unit: $q \times 10^{-3}/m_{\pi^+}^2$) with statistical and systematic errors in comparison to the predictions of ChPT [8,19] ($\mathcal{O}(p^3)$) and of a dispersion theoretical approach (DR, [17]).

	This work		ChPT	DR ^a
	qk -fit ^a	q -fit		
$E_{0+}(E_{\text{thr}}^{p\pi^0})$	$-1.23 \pm 0.08 \pm 0.03$	$-1.33 \pm 0.08 \pm 0.03$	-1.16	-1.22
$E_{0+}(E_{\text{thr}}^{n\pi^+})$	$-0.45 \pm 0.07 \pm 0.02$	$-0.45 \pm 0.06 \pm 0.02$	-0.43	-0.56
β	$2.43 \pm 0.28 \pm 1.0$	$5.2 \pm 0.2 \pm 1.0$	2.78	3.6
P_1	$9.46 \pm 0.05 \pm 0.28$	$9.47 \pm 0.08 \pm 0.29$	9.14 ± 0.5	9.55
P_2	$-9.5 \pm 0.09 \pm 0.28$	$-9.46 \pm 0.1 \pm 0.29$	-9.7 ± 0.5	-10.37
P_3	$11.32 \pm 0.11 \pm 0.34$	$11.48 \pm 0.06 \pm 0.35$	10.36	9.27
P_{23}	10.45 ± 0.07	10.52 ± 0.06	11.07	9.84

^aValues of the P -wave combinations converted into the unit $q \times 10^{-3}/m_{\pi^+}^2$.

P -wave low-energy theorems. This gives confidence in the third-order LET predictions for P_1 and P_2 , which are in agreement with the present MAMI data. With the new value of b_P [20], fitted to the present MAMI data, the ChPT calculation is in agreement with the measured photon asymmetry.

2. The $\gamma N \rightarrow \Delta(1232)$ transition and the E2/M1 ratio

Low energy electromagnetic properties of baryons, such as mass, charge radius, magnetic and quadrupole moments are important observables for any model of the nucleon structure. In various constituent-quark models a tensor force in the inter-quark hyperfine interaction, introduced first by de Rujula, Georgi and Glashow [21], leads to a d -state admixture in the baryon ground-state wave-function. As a result the tensor force induces a small violation of the Becchi–Morpurgo selection rule [22], that the $\gamma N \rightarrow \Delta(1232)$ excitation is a pure M1 (magnetic dipole) transition, by introducing a non-vanishing E2 (electric quadrupole) amplitude. For chiral quark models or in the Skyrmon picture of the nucleon, the main contribution to the E2 strength stems from tensor correlations between the pion cloud and the quark bag, or meson exchange currents between the quarks. To observe a static deformation (d -state admixture) a target with a spin of at least $3/2$ (*e.g.* Δ matter) is required. The only realistic alternative is to measure the transition E2 moment in the $\gamma N \rightarrow \Delta$ transition at resonance, or equivalently the $E_{1+}^{3/2}$ partial wave amplitude in the $\Delta \rightarrow N\pi$ decay. The experimental quantity of interest to compare with the different nucleon models is the ratio $R_{EM} = E2/M1 = E_{1+}^{3/2}/M_{1+}^{3/2}$ of the electric quadrupole E2 to the magnetic dipole M1 amplitude in the region of the $\Delta(1232)$ resonance. In quark models with SU(6) symmetry, for example the MIT bag model, $R_{EM} = 0$ is predicted. Depending on the size of the hyperfine interaction and the bag radius, broken SU(6) symmetry leads to $-2\% < R_{EM} < 0$ [23–26]. Larger negative values in the range $-6\% < R_{EM} < -2.5\%$ have been predicted by Skyrme models [27] while results from chiral bag models [28] give values in the range -2% to -3% . The first Lattice QCD result is $R_{EM} = (+3 \pm 9)\%$ [29] and a quark model with exchange currents yields values of about -3.5% [30].

The determination of the quadrupole strength E2 in the region of the $\Delta(1232)$ resonance has been the aim of a considerable number of experiments and theoretical activities in the last few years. Experimental results have been published for the differential cross section and photon asymmetry of pion photoproduction off the proton from the Mainz Microtron MAMI and the laser backscattering facility LEGS at Brookhaven National Laboratory, with the results $R_{EM} = -(2.5 \pm 0.2_{\text{stat.}} \pm 0.2_{\text{sys.}})\%$ from the Mainz group [31] and $R_{EM} = -(3.0 \pm 0.3_{\text{stat.} + \text{sys.}} \pm 0.2_{\text{mod}})\%$ from the LEGS group [32]. These

new R_{EM} results have started intense discussions about the correct way to extract the E2/M1 ratio from the new experimental data. In particular the large variation in the R_{EM} values obtained in theoretical analysis of these data at RPI [33] ($R_{EM} = -(3.2 \pm 0.25)\%$), VPI [34] ($R_{EM} = -(1.5 \pm 0.5)\%$) and Mainz [35] ($R_{EM} = -(2.5 \pm 0.1)\%$) was quite unsatisfactory. Since small differences in the differential cross section occur in the mentioned MAMI/DAPHNE and LEGS experiments, a new experiment on neutral pion photoproduction off the proton has been performed at the Mainz Microtron covering the full polar angle range of the pion. The new enlarged set of experimental results should allow a determination of R_{EM} more accurately.

2.1. New experimental results for $\gamma N \rightarrow \Delta(1232)$

Figure 4 shows the new results for the photon asymmetry for six different energies in the Δ -resonance region. For the first time this new experiment delivers data in the full polar angle range. The new results are in good agreement with the experimental data of MAMI/DAPHNE and LEGS. In addition, the photon asymmetries of all three experiments are compared to the dispersion theoretical analysis of Hanstein [35,36] and good agreement is found.

The unpolarized differential cross sections for the same six photon energies in the Δ -resonance region are shown in figure 5. The new results are in agreement with the MAMI/DAPHNE, the LEGS data differ not only in the absolute values of the differential cross section but show as well a different angular distribution. In addition, the results of the Hanstein analysis for the MAMI/TAPS data are shown.

In the angular momentum expansion of the neutral pion photoproduction it is sufficient to take into account s - and p -waves, *i.e.* $l_\pi = 0$ or 1 only. The angular distributions for the unpolarized cross section $d\sigma_0/d\Omega$, the parallel part $d\sigma_{||}/d\Omega$ (pion detected in the plane defined by the photon polarization and the photon momentum vector), and perpendicular part $d\sigma_{\perp}/d\Omega$ can be expressed in the s - and p -wave approximation by the parameterization

$$\frac{d\sigma_j(\theta)}{d\Omega} = \frac{q}{k} (A_j + B_j \cos(\theta) + C_j \cos^2(\theta)) , \quad (4)$$

where q and k denote the center of mass momenta of the pion and the photon, respectively, and j indicates the parallel ($||$), perpendicular (\perp) and unpolarized (0) components. The coefficients A_j , B_j and C_j are quadratic or bilinear functions of the s - and p -wave amplitudes. In particular, $d\sigma_{||}/d\Omega$ is sensitive to the E_{1+} amplitude, because of interference with M_{1+} in the terms

$$A_{||} = |E_{0+}|^2 + |3E_{1+} - M_{1+} + M_{1-}|^2 , \quad (5)$$

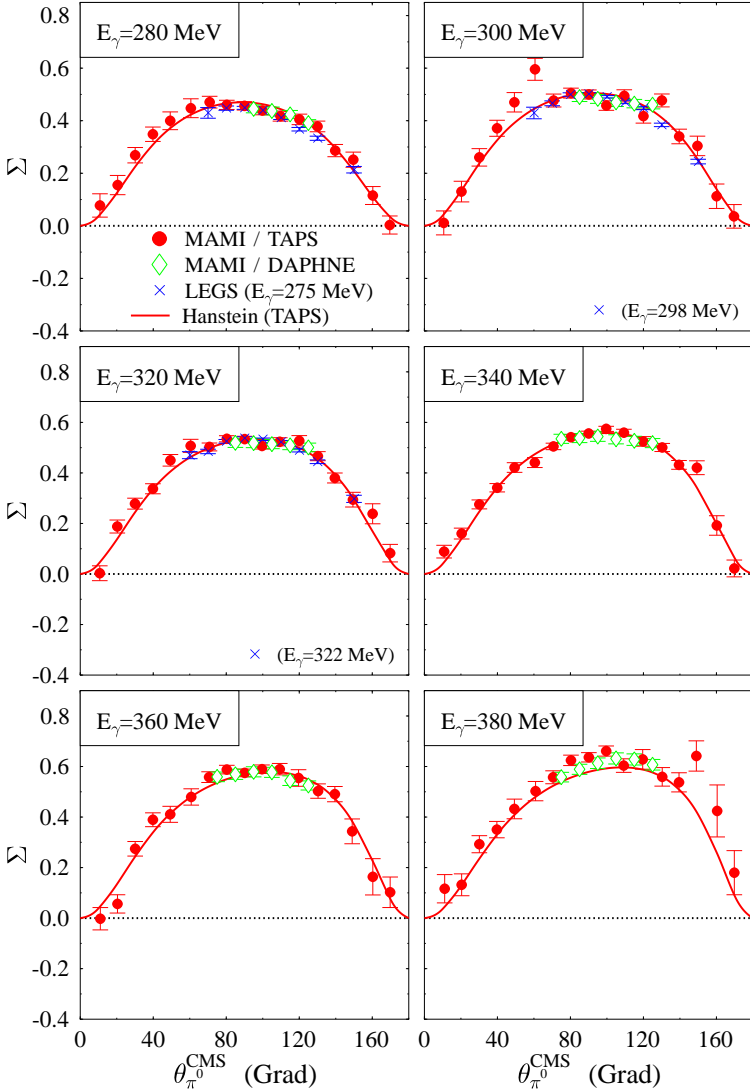


Fig. 4. Photon asymmetries Σ in the Δ -resonance region (solid circles, this work Ref. [38], open diamonds Ref. [31] and crosses Ref. [32]).

$$B_{\parallel} = 2\text{Re}[E_{0+}(3E_{1+} + M_{1+} - M_{1-})^*], \quad (6)$$

$$C_{\parallel} = 12\text{Re}[E_{1+}(M_{1+} - M_{1-})^*]. \quad (7)$$

Furthermore, the ratio

$$R = \frac{1}{12} \frac{C_{\parallel}}{A_{\parallel}} = \frac{\text{Re}(E_{1+}(M_{1+} - M_{1-})^*)}{|E_{0+}|^2 + |3E_{1+} + M_{1+} - M_{1-}|^2} \quad (8)$$

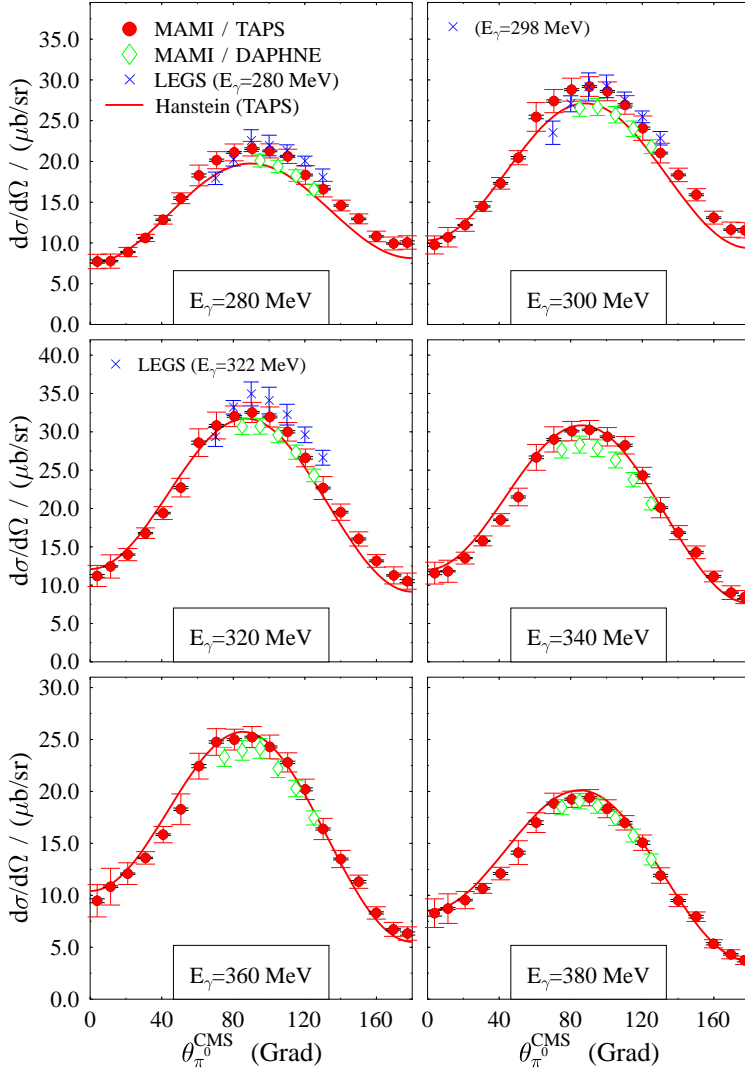


Fig. 5. Differential cross sections in the Δ -resonance region. MAMI/TAPS results are shown with statistical (1–2 %) and systematic errors (solid circles, this work Ref. [38], open diamonds Ref. [31] and crosses Ref. [32])

can be identified with the ratio $R_{EM} = E_{1+}^{3/2}/M_{1+}^{3/2}$ at the $\Delta(1232)$ resonance ($\delta_{33} = 90^\circ$)

$$R \simeq R_{EM} = \left. \frac{\text{Im } E_{1+}^{3/2}}{\text{Im } M_{1+}^{3/2}} \right|_{W=M_\Delta}. \quad (9)$$

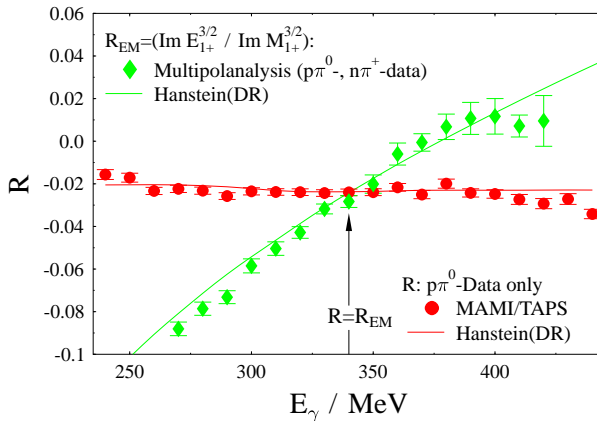


Fig. 6. The energy dependence of the ratio $E_{1+}^{3/2}/M_{1+}^{3/2}$ is shown as solid diamonds. In addition, the energy dependence of $R = C_{\parallel}/(12A_{\parallel})$ is shown as solid squares.

This is the crucial point of our analysis [37]. This method offers the advantage of being independent of absolute normalization and insensitive to many systematic errors, because R_{EM} is extracted from the ratio of the coefficients C_{\parallel} and A_{\parallel} fitted to the angular distribution of $d\sigma_{\parallel}/d\Omega$. Further, the following identity can be derived [38]:

$$R = \frac{1}{12} \frac{C_{\parallel}}{A_{\parallel}} = \frac{1}{12} \frac{C}{A} + \frac{\Sigma(\theta = 90^\circ)}{1 - \Sigma(\theta = 90^\circ)} \approx R_{EM} \quad (10)$$

which depends only on the shape (C/A) of the differential cross section $d\sigma/d\Omega$ and the photon asymmetry Σ at $\theta^{CMS} = 90^\circ$. Using equation (10), the ratio R_{EM} can be extracted [38]

$$R_{EM} = (-2.4 \pm 0.16_{\text{stat.}} \pm 0.24_{\text{sys.}}) \% \quad (11)$$

According to the Fermi–Watson theorem the $E_{1+}^{3/2}$ and $M_{1+}^{3/2}$ partial waves have the same phase δ_{33} and the ratio $E_{1+}^{3/2}/M_{1+}^{3/2}$ is real quantity. As shown in Fig. 6, this ratio is strongly dependent on the photon energy and varies from -8% at $E_\gamma = 270$ MeV to $+2\%$ at $E_\gamma = 420$ MeV.

3. Future plans with real photons at MAMI

We propose to use the intense, high quality, ultra-fine tagged, linearly and circularly polarized photon beams of MAMI together with a 4π multi-photon spectrometer (Crystal Ball + TAPS) and a proton target (polarized and unpolarized) to perform a series of precision experiments on non-perturbative QCD. We intend to make sensitive tests of Chiral perturbation

theory, effective Lagrangian models such as the flux-tube quark model and various Lattice QCD computations. Highlights of the program include:

- threshold strangeness and threshold ω production,
- $\eta, \omega, 3\pi^0, 2\pi^0, \pi^0$ production to measure the radiative couplings of N^* and Δ resonances,
- radiative pion production to determine the magnetic dipole moment of the $\Delta^+(1232)$ resonance; also radiative η production to measure the magnetic dipole moment of the $S_{11}(1535)$ state,
- a double polarization experiment of linearly polarized photons on a longitudinally polarized proton target. This is a unique probe of the Roper resonance $P_{11}(1440)$.

Furthermore we plan to investigate:

- Meson photoproduction reactions of a neutron target using a deuterium target.
- Compton scattering with polarized beams and targets.
- $2\pi^0, \eta$ and ω production on complex targets to investigate medium modifications.
- Coherent π^0 production on heavy nuclear targets to study nuclear radii.

The Crystal Ball, CB, spectrometer consists of a highly segmented sphere made of NaI. The sphere has an entrance and exit tunnel for the beam and a spherical cavity for the liquid hydrogen target, see Fig. 7. The target is surrounded by a cylinder of scintillation counters that function as the charged particle veto. The solid angle of the CB is 93 % of 4π steradian. The Crystal Ball was built at SLAC and used in J/ψ measurements at SPEAR and b -quark physics at DESY.

The CB is constructed of 672 optically isolated NaI(Tl) crystals, 15.7 radiation lengths thick. The counters are arranged in a spherical shell with an inner radius of 25.3 cm and an outer radius of 66.0 cm. The hygroscopic NaI is housed in two hermetically sealed evacuated hemispheres. The CB geometry is based on that of an icosahedron. Each of the 20 triangular faces (“major triangles”) is divided into four “minor triangles”, each consisting of nine separate crystals. Each crystal is shaped like a truncated triangular pyramid, 40.6 cm high, pointing towards the center of the Ball. The sides on the inner end are 5.1 cm long and 12.7 cm on the far end, see Fig. 7. Each

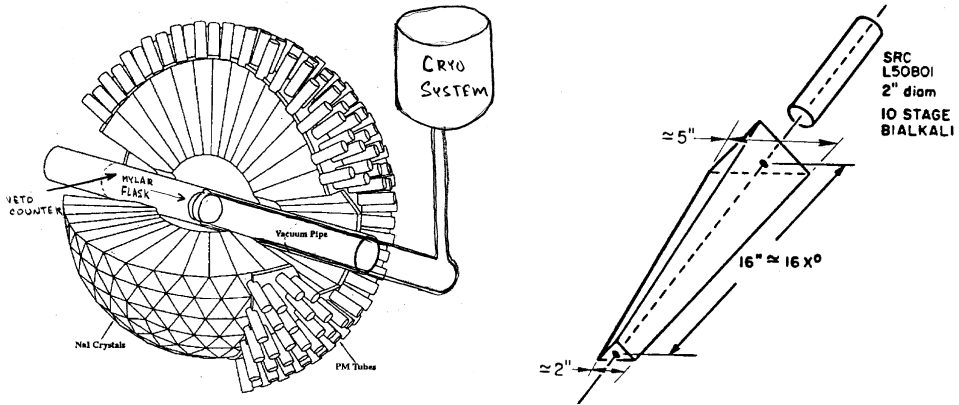


Fig. 7. Left: The Crystal Ball detector. Right: Typical Crystal Ball crystal.

crystal is individually wrapped in reflector paper and aluminized mylar; it is viewed by its own a 5.1 cm diameter SRC L50 B01 photomultiplier, selected for linearity over a wide dynamic range. The phototube is separated from the crystal by a glass window and a 5 cm air gap. The crystals have been stacked so as to form two mechanically separate top and bottom hemispheres. The boundary between the two hemispheres is called the equator region. It is ~ 0.8 cm thick, consisting of two 1.6 mm stainless steel plates separated by 5 mm of air. This introduces an inactive space amounting to 1.6% of the solid angle. The inner wall of the hemisphere is 1.5 mm stainless steel or 0.09 r.l. The Ball has an entrance and exit opening for the beam which results in a loss of 4.4% of acceptance.

This work is supported by Deutsche Forschungsgemeinschaft (SFB 201 and SFB 443).

REFERENCES

- [1] E. Mazzucato *et al.*, *Phys. Rev. Lett.* **57**, 3144 (1986).
- [2] R. Beck *et al.*, *Phys. Rev. Lett.* **65**, 1841 (1990).
- [3] M. Fuchs *et al.*, *Phys. Lett.* **B368**, 20 (1996).
- [4] J.C. Bergstrom *et al.*, *Phys. Rev.* **C53**, R1052 (1996); *Phys. Rev.* **C55**, 2016 (1997).
- [5] P. de Baenst, *Nucl. Phys.* **B24**, 633 (1970).
- [6] I.A. Vainshtein, V.I. Zakharov, *Nucl. Phys.* **B36**, 589 (1972).
- [7] V. Bernard, J. Gasser, N. Kaiser, U.-G. Meißner, *Phys. Lett.* **B268**, 291 (1991).

- [8] V. Bernard, N. Kaiser, U.-G. Meißner, *Z. Phys.* **C70**, 483 (1996).
- [9] A. Schmidt, Doktorarbeit, University Mainz, (2001).
- [10] H. Herminghaus, K.H. Kaiser, H. Euteneuer, *Nucl. Instrum. Methods Phys. Res.* **A138**, 1 (1976).
- [11] I. Anthony *et al.*, *Nucl. Instrum. Methods Phys. Res.* **A301**, 230 (1991).
- [12] S.J. Hall *et al.*, *Nucl. Instrum. Methods Phys. Res.* **A368**, 698 (1996).
- [13] R. Novotny, *IEEE Trans. Nucl. Sci.* **38**, 379 (1991).
- [14] D. Lohmann, J. Peise *et al.*, *Nucl. Instrum. Methods Phys. Res.* **A343**, 494 (1994).
- [15] A. Schmidt, Diplomarbeit, University Mainz (1995).
- [16] R. Novotny, *IEEE Trans. Nucl. Sci.* **43**, 1260 (1996).
- [17] O. Hanstein, D. Drechsel, L. Tiator, *Phys. Lett.* **B399**, 13 (1997).
- [18] A. Schmidt *et al.*, *Phys. Rev. Lett.* **87**, 232501 (2001).
- [19] V. Bernard, N. Kaiser, U.-G. Meißner, *Phys. Lett.* **B378**, 337 (1996).
- [20] V. Bernard, N. Kaiser, U.-G. Meißner, *Eur. Phys. J.* **A11**, 209 (2001).
- [21] A. Rujula, H. Georgi, S.L. Glashow, *Phys. Rev.* **D12**, 147 (1975).
- [22] C. Becchi, G. Morpurgo, *Phys. Lett.* **17**, 352 (1965).
- [23] R. Koniuk, N. Isgur, *Phys. Rev.* **D21**, 1868 (1980).
- [24] S.S. Gershteyn *et al.*, *Sov. J. Nucl. Phys.* **34**, 870 (1981).
- [25] D. Drechsel, M.M. Giannini, *Phys. Lett.* **B143** 329 (1984).
- [26] S. Capstick, *Phys. Rev.* **D46**, 2864 (1992).
- [27] A. Wirzba, W. Weise, *Phys. Lett.* **B188**, 6 (1987).
- [28] K. Bermuth *et al.*, *Phys. Rev.* **D37**, 89 (1988).
- [29] D.B. Leinweber, *Proc. Int. Conf. "Baryons92"*, 1992, p. 29.
- [30] A. Buchmann *et al.*, *Phys. Rev.* **C55**, 448 (1997).
- [31] R. Beck, H.-P. Krahn *et al.*, *Phys. Rev. Lett.* **78**, 606 (1997).
- [32] G.S. Blanpied *et al.*, *Phys. Rev. Lett.* **79**, 4337 (1997).
- [33] R.M. Davidson, N.C. Mukhopadhyay, *Phys. Rev. Lett.* **79**, 4509 (1997).
- [34] G. Keaton, R.L. Workman, *Phys. Rev. Lett.* **79**, 4511 (1997).
- [35] O. Hanstein *et al.*, *Phys. Lett.* **B385**, 45 (1996).
- [36] O. Hanstein *et al.*, *Nucl. Phys.* **A632**, 561 (1998).
- [37] R. Beck *et al.*, *Phys. Rev.* **C61**, 035204 (2000).
- [38] R. Leukel, PhD thesis, University Mainz, 2001.